

Longitudinal polarization periodicity of unpolarized light passing through a double wedge depolarizer

Juan Carlos G. de Sande,¹ Massimo Santarsiero,^{2,*} Gemma Piquero,³
and Franco Gori²

¹*Departamento de Circuitos y Sistemas, Universidad Politécnica de Madrid, 28031 Madrid, Spain*

²*Dipartimento di Fisica, Università Roma Tre, and CNISM, via della Vasca Navale 84, I-00146 Roma, Italy*

³*Departamento de Óptica, Universidad Complutense de Madrid, 28040 Madrid, Spain*

[*santarsiero@fis.uniroma3.it](mailto:santarsiero@fis.uniroma3.it)

Abstract: The polarization characteristics of unpolarized light passing through a double wedge depolarizer are studied. It is found that the degree of polarization of the radiation propagating after the depolarizer is uniform across transverse planes after the depolarizer, but it changes from one plane to another in a periodic way giving, at different distances, unpolarized, partially polarized, or even perfectly polarized light. An experiment is performed to confirm this result. Measured values of the Stokes parameters and of the degree of polarization are in complete agreement with the theoretical predictions.

© 2012 Optical Society of America

OCIS codes: (260.5430) Polarization; (030.1640) Coherence (240.5440); Polarization-selective devices.

References and links

1. J. P. McGuire and R. A. Chipman, "Analysis of spatial pseudodepolarizers in imaging systems," *Opt. Eng.* **29**, 1478–1484 (1990).
2. S. C. McClain, R. A. Chipman, and L. W. Hillman "Aberrations of a horizontal/vertical depolarizer," *Appl. Opt.* **31**, 2326–2331 (1992).
3. M. El Sherif, M.S. Khalil, S. Khodeir, and N. Nagib, "Simple depolarizers for spectrophotometric measurements of anisotropic samples," *Opt. & Laser Technol.* **28**, 561–563 (1996).
4. G. Biener, A. Niv, V. Kleiner, and E. Hasman, "Computer-generated infrared depolarizer using space-variant subwavelength dielectric gratings," *Opt. Lett.* **28**, 1400–1402 (2003).
5. V. A. Bagan, B. L. Davydov, and I. E. Samartsev, "Characteristics of Cornu depolarisers made from quartz and paratellurite optically active crystals," *Quant. Electron.* **39**, 73–78 (2009).
6. C. Vena, C. Versace, G. Strangi, and R. Bartolino, "Light depolarization by non-uniform polarization distribution over a beam cross section," *J. Opt. A: Pure Appl. Opt.* **11**, 125704–10 (2009).
7. J. C. G. de Sande, G. Piquero, and C. Teijeiro, "Polarization changes at Lyot depolarizer output for different types of input beams," *J. Opt. Soc. Am. A* **29**, 278–284 (2012).
8. F. Gori, M. Santarsiero, S. Vicalvi, and R. Borghi, "Beam coherence-polarization matrix," *Pure and Appl. Opt.* **7**, 941–951 (1998).
9. F. Gori, M. Santarsiero, R. Borghi, and G. Guattari, "The irradiance of partially polarized beams in a scalar treatment," *Opt. Commun.* **163**, 159–163 (1999).
10. G. P. Agrawal and E. Wolf, "Propagation-induced polarization changes in partially coherent optical beams," *J. Opt. Soc. Am. A* **17**, 2019–2023 (2000).
11. E. Wolf, "Unified theory of coherence and polarization of random electromagnetic beams," *Phys. Lett. A* **312**, 263–267 (2003).

12. F. Gori, M. Santarsiero, R. Borghi, and E. Wolf, "Effects of coherence on the degree of polarization in a Young interference pattern," *Opt. Lett.* **31**, 688–690 (2006).
13. M. Salem and E. Wolf "Coherence-induced polarization changes in light beams," *Opt. Lett.* **33**, 1180–1182 (2008).
14. T. D. Visser, D. Kuebel, M. Lahiri, T. Shirai, and E. Wolf, "Unpolarized light beams with different coherence properties," *J. Mod. Opt.* **56**, 1369–1374 (2009).
15. F. Gori, J. Tervo, and J. Turunen, "Correlation matrices of completely unpolarized beams," *Opt. Lett.* **34**, 1447–1449 (2009).
16. R. Martínez-Herrero and P. M. Mejías, "On the propagation of random electromagnetic fields with position-independent stochastic behavior," *Opt. Commun.* **283**, 4467–4469 (2010).
17. H. Lotem and U. Taor, "Low-loss bireflectant (double reflection) polarization prism," *Appl. Opt.* **25**, 1271–1273 (1985).
18. L. V. Alekseeva, I. V. Povkh, V. I. Stroganov, B. I. Kidyarov, and P. G. Pasko, "Four-ray splitting in optical crystals," *J. Opt. Technol.* **39**, 441–443 (2002).
19. V. Kuznetsov, D. Faleiev, E. Savin, and V. Lebedev, "Crystal-based device for combining light beams," *Opt. Lett.* **34**, 2856–2857 (2009).
20. E. Wolf, *Introduction to the Theory of Coherence and Polarization of Light* (Cambridge University Press, Cambridge, 2007).
21. S. C. McClain, L. W. Hillman, and R. A. Chipman, "Polarization ray tracing in anisotropic optically active media. II. Theory and physics," *J. Opt. Soc. Am. A* **10**, 2383–2393 (1993).
22. M. Born and E. Wolf, *Principles of Optics* (Cambridge U. Press, 7th expanded, Cambridge, 1999).
23. F. Gori, "Measuring Stokes parameters by means of a polarization grating," *Opt. Lett.* **24**, 584–586 (1999).
24. G. Piquero, R. Borghi, and M. Santarsiero, "Gaussian Schell-model beams propagating through polarization gratings," *J. Opt. Soc. Am. A* **18**, 1399–1405 (2001).
25. H. F. Talbot, "Facts relating to optical science," *Phil. Mag.* **9**, 401–407 (1836).
26. V. Arrizón, E. Tepichin, M. Ortiz-Gutiérrez, and A.W. Lohmann, "Fresnel diffraction at 1/4 of the Talbot distance of an anisotropic grating," *Opt. Commun.* **127**, 171–175 (1996).
27. J. Tervo and J. Turunen, "Transverse and longitudinal periodicities in fields produced by polarization gratings," *Opt. Commun.* **190**, 51–57 (2001).
28. Z. Bomzon, A. Niv, G. Biener, V. Kleiner, and E. Hasman, "Polarization Talbot self-imaging with computer-generated, space-variant subwavelength dielectric gratings," *Appl. Opt.* **41**, 5218–5222 (2002).
29. S. C. McClain, L. W. Hillman, and R. A. Chipman, "Polarization ray tracing in anisotropic optically active media. I. Algorithms," *J. Opt. Soc. Am. A* **10**, 2371–2382 (1993).
30. Z. Zhang and H. J. Caulfield, "Reflection and refraction by interfaces of uniaxial crystals," *Opt. & Laser Technol.* **28**, 549–553 (1996).
31. G. Ghosh, "Dispersion-equation coefficients for the refractive index and birefringence of calcite and quartz crystals," *Opt. Commun.* **163**, 95–102 (1999).

1. Introduction

The use of optical devices that reduce the degree of polarization (DOP) of light is necessary for removing undesired polarization effects that could affect the performance of many optical systems, [1–7]. Approaches for reducing the DOP are based on scrambling states of polarization either in time, wavelength or space domain. One commercially available spatial polarization-state scrambler or *pseudo-depolarizer* is the double wedge depolarizer (DWD), which consists of a pair of uniaxial crystal wedges, with suitably oriented optic axes, placed in contact to form a plate. When a totally and uniformly polarized light impinges on it, this kind of elements produces a periodic variation of the state of polarization across a plane parallel to the output face of the device. The DOP at any point is equal to one but when the Stokes parameters are integrated over a large area compared to the period of the state of polarization, it becomes nearly zero.

The polarization characteristics of the radiation produced by a depolarizer are usually analyzed only at the exit face of the device [1–6], considering perfectly polarized incident light. In the present paper the output field is analyzed at a generic distance from the exit face of the DWD and the incident light is supposed to be unpolarized. A somewhat unexpected result is obtained: under free propagation after the DWD, the DOP is uniform (as well as the intensity profile) across any transverse plane (with respect to the mean propagation direction) but it

changes from one plane to another in a periodic way, giving rise to unpolarized or completely polarized light although with nonuniform polarization at different equally spaced z -positions.

This “polarizing” property of DWD’s, besides its interest in connection with the recent research on the relationship between coherence and polarization of propagating fields [8–16], could be exploited for synthesizing transversally periodic polarization structures, whose DOP can be varied at will, on changing the propagation distance beyond the device.

The work is organized as follows. In Sec. 2 the theoretical analysis is presented, pertinent to the case of a monochromatic plane wave incident orthogonally on the input face of the DWD. In particular, the polarization characteristics of the output radiation are first studied when the incident wave is perfectly polarized and then the obtained results are used to study unpolarized light. The performed experiment is described in Sec. 3, where the obtained results are compared to the theoretical predictions as well. Finally, the main conclusions of this work are summarized in Sec. 4. In an Appendix some details of the calculations of the fields of Sec. 2 are reported.

2. Theory

2.1. Preliminaries

The geometry of the problem is shown in Fig. 1(a). The reference frame is chosen in such a way that the z axis is orthogonal to the faces of the device (with origin at its exit face) and the thickness of the wedges varies along the x axis. The first wedge has its optic axis along the y direction and thickness (at $x = 0$) equal to d_1 . The second wedge has thickness d_2 (at $x = 0$) and its optic axis is in the xy plane and forms an angle of 45° with respect to the first one.

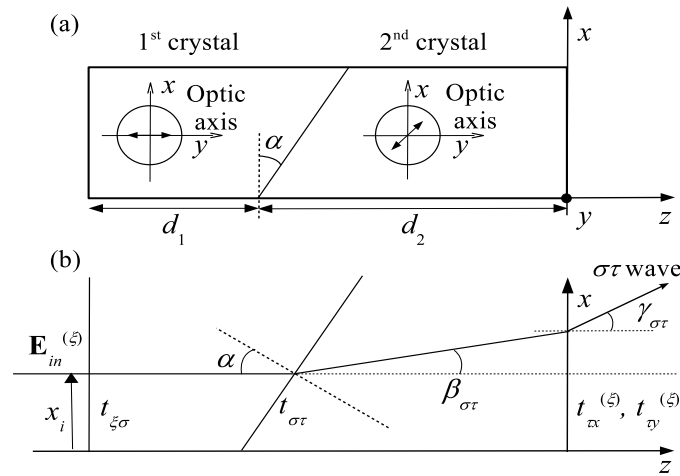


Fig. 1. (a) Schematic sketch of a DWD; (b) notations used throughout the paper.

It is well known that, when an arbitrarily polarized beam impinges onto the separation surface of two uniaxial crystals with their optic axes arbitrarily oriented, up to four refracted (and four reflected) beams are produced [17–19]. Now we will derive the propagation directions and the corresponding amplitudes of the four plane waves that are produced when an arbitrary polarized monochromatic plane wave impinges orthogonally on a DWD. We will first consider the case

of a totally polarized input wave. The obtained results will be used to study the case of a completely unpolarized input wave.

Light fields will be considered that mostly propagate along the z axis, so that they can be characterized through their Jones vector, defined as [20]

$$\mathbf{E}(\mathbf{r}) = \begin{pmatrix} E_x(\mathbf{r}) \\ E_y(\mathbf{r}) \end{pmatrix}, \quad (1)$$

where E_x and E_y are the components of the electric field along the x and y axes, at the typical point \mathbf{r} . In the most general case, the quantities appearing in the Jones vector are stochastic variables and the polarization characteristics are described through the correlation functions among all the transverse field components. Such correlation functions are collected into the polarization matrix, i.e.,

$$\hat{P}(\mathbf{r}) = \langle \mathbf{E}(\mathbf{r}) \mathbf{E}^\dagger(\mathbf{r}) \rangle, \quad (2)$$

with the dagger representing hermitian conjugation and $\langle \cdot \rangle$ the ensemble average. The total intensity of the field is defined as the trace of \hat{P} , while the local degree of polarization (DOP) is evaluated as

$$p(\mathbf{r}) = \sqrt{1 - \frac{4 \text{Det}\{\hat{P}(\mathbf{r})\}}{\text{Tr}^2\{\hat{P}(\mathbf{r})\}}}. \quad (3)$$

Since the matrix \hat{P} is hermitian and semipositive defined, the DOP only assumes values in the interval $[0, 1]$, $p = 1$ corresponding to a perfectly polarized field and $p = 0$ to a completely unpolarized one.

The polarization properties of the light fields will be described through the Stokes vector, that conveys the same information content as the polarization matrix, and whose elements are related to the elements of the latter by the relations

$$\mathbf{s}(\mathbf{r}) = \begin{pmatrix} s_0(\mathbf{r}) \\ s_1(\mathbf{r}) \\ s_2(\mathbf{r}) \\ s_3(\mathbf{r}) \end{pmatrix} = \begin{pmatrix} P_{xx}(\mathbf{r}) + P_{yy}(\mathbf{r}) \\ P_{xx}(\mathbf{r}) - P_{yy}(\mathbf{r}) \\ 2 \text{Re}\{P_{yx}(\mathbf{r})\} \\ 2 \text{Im}\{P_{yx}(\mathbf{r})\} \end{pmatrix}, \quad (4)$$

where $s_0(\mathbf{r})$ is the intensity while the three remaining parameters represent the state of polarization.

2.2. Totally polarized input light

In order to study the field transmitted by the DWD with a totally polarized input plane wave, we will consider separately two impinging plane waves, propagating along the z axis with uniform and linear polarization along the x and the y direction, respectively. In Fig. 1(b) the notations used in the following are introduced. In particular, the wave-vector direction of a typical plane wave propagating in each medium is shown, together with the transmission coefficients at each interface. Note that, due to the used geometry, the wave vectors of all waves lie in the xz plane. The superscript ($\xi = x, y$), when it occurs, always refers to the original polarization of the wave impinging on the device. The first subindex of the transmission coefficients refers to the polarization direction of the field in the incidence medium: x or y , if the incidence medium is air, o or e (from ordinary and extraordinary, respectively) if the incidence medium is the crystal. The same convention holds for the second subindex, but referred to the transmission medium. The angle that each wave vector inside the second wedge forms with the z axis will be referred to as $\beta_{\sigma\tau}$, where $\sigma = o, e$ denotes the character (ordinary or extraordinary) of the wave in the first wedge and $\tau = o, e$ denotes the character of the wave in the second wedge. Finally,

$\gamma_{\sigma\tau}$ denotes the refraction angle of the corresponding $\sigma\tau$ wave at the exit surface. Due to the geometry of the DWD, all the waves propagate forming large angles with respect to the optic axes of the crystals. As a consequence, the effects of optical activity can be neglected [21].

Let us first consider an impinging plane wave linearly polarized along the x direction. Its Jones vector is of the form

$$\mathbf{E}_{in}^{(x)} = A \begin{pmatrix} 1 \\ 0 \end{pmatrix}, \quad (5)$$

where A is the amplitude of the field across the input face of the DWD and in stands for input.

Assuming that all the fields have a negligible z -component, the Jones vector of the output field, $\mathbf{E}_{out}^{(x)}$, across a typical plane $z > 0$ can be evaluated taking the effects of all interfaces and propagation distances into account. After some calculations, it turns out to be (see Appendix)

$$\mathbf{E}_{out}^{(x)}(x, z) = \frac{A}{\sqrt{2}} t_{xo} a_{oo}(z) \left[t_{oo} \begin{pmatrix} t_{ox}^{(x)} \\ -t_{oy}^{(x)} \end{pmatrix} + t_{oe} \begin{pmatrix} t_{ex}^{(x)} \cos \gamma_{oe} \\ t_{ey}^{(x)} \end{pmatrix} \exp[-i\delta_o(x, z)] \right], \quad (6)$$

with

$$a_{oo}(z) = \exp(-ik_o d - ikz) \quad (7)$$

and

$$\delta_o(x, z) = d_2 (k_{oe} \cos \beta_{oe} - k_o) + xk \sin \gamma_{oe} - zk(1 - \cos \gamma_{oe}). \quad (8)$$

Here, $d = d_1 + d_2$ is the total thickness of the device, k is the vacuum wave number, k_o is the ordinary wave number and k_{oe} is the wave number corresponding to the oe extraordinary wave. This wave number, as well as the angles β_{oe} and γ_{oe} , can be calculated by repeatedly applying the Snell law, together with the relation

$$\frac{1}{k_{oe}^2} = \frac{\sin^2 \varphi}{k_e^2} + \frac{\cos^2 \varphi}{k_o^2}, \quad (9)$$

obtained from the index ellipse for a wave travelling at an angle φ with respect to the optic axis of the second wedge [22].

Equations (6), (7) and (8) state that the output field consists of two plane waves, having different amplitudes, propagation directions and polarization states. The first one (oo) propagates along the z axis, while the other one (oe) propagates along a direction that forms the angle γ_{oe} with respect to the z axis. Since the transmission coefficients are real quantities, the polarizations of the two waves are linear, but directed along different directions. The sum of such two waves produces a periodic variation of the polarization state across the transverse plane, with period $L_o = 2\pi/(k|\sin \gamma_{oe}|)$, in a similar way to that generated by a polarization grating [23, 24]. According to the Talbot effect [25], applied to transverse modulations of the polarization state [26–28], a longitudinal periodicity of the polarization transverse pattern is expected with period $z_T = 2L_o^2/\lambda$.

A simpler expression is obtained if one considers the given optic-axis orientations and that the wedge angle α is typically small. In such cases, the following approximations hold [21, 29, 30]:

$$T_x \equiv t_{xo} t_{oo} t_{ox}^{(x)} = t_{xo} t_{oo} t_{oy}^{(x)} \simeq t_{xo} t_{oe} t_{ex}^{(x)} \cos \gamma_{oe} \simeq t_{xo} t_{oe} t_{ey}^{(x)}, \quad (10)$$

and the output field can be written as

$$\mathbf{E}_{out}^{(x)}(x, z) \simeq \frac{A}{\sqrt{2}} T_x a_{oo}(z) \left[\begin{pmatrix} 1 \\ -1 \end{pmatrix} + \begin{pmatrix} 1 \\ 1 \end{pmatrix} \exp[-i\delta_o(x, z)] \right]. \quad (11)$$

From Eq. (11) it is deduced that the amplitudes of the two produced plane waves are equal, while their polarizations are mutually orthogonal. More precisely, the oo plane wave, which

propagates along the z axis, is linearly polarized at -45° , while the other one (oe) is linearly polarized at $+45^\circ$. Therefore, the polarization state across a transverse plane periodically varies along the x axis, from linear to circular and vice versa, with a period depending on the angle between the two propagation directions. This is at the basis of the use of such a device as a “depolarizer”: although the local degree of polarization must be unitary at every point, it vanishes when the average polarization is considered over spatial regions having size much larger than the transverse period of polarization state.

Let us now consider an incident monochromatic plane wave uniformly and linearly polarized along the y direction. In this case the Jones vector is given by

$$\mathbf{E}_{in}^{(y)} = A \begin{pmatrix} 0 \\ 1 \end{pmatrix}. \quad (12)$$

On proceeding as for the previous case, at a typical plane $z > 0$ the Jones vector turns out to be

$$\mathbf{E}_{out}^{(y)}(x, z) = \frac{A}{\sqrt{2}} t_{ye} a_{ee}(x, z) \left[t_{ee} \begin{pmatrix} t_{ex}^{(y)} \cos \gamma_{ee} \\ t_{ey}^{(y)} \end{pmatrix} + t_{eo} \begin{pmatrix} -t_{ox}^{(y)} \cos \gamma_{eo} \\ t_{oy}^{(y)} \end{pmatrix} \exp[-i\delta_e(x, z)] \right] \quad (13)$$

with

$$a_{ee}(x, z) = \exp(-ik_e d_1 - ik_{ee} d_2 \cos \beta_{ee} - ikx \sin \gamma_{ee} - ikz \cos \gamma_{ee}) \quad (14)$$

and

$$\delta_e(x, z) = d_2 (k_o \cos \beta_{eo} - k_{ee} \cos \beta_{ee}) + xk (\sin \gamma_{eo} - \sin \gamma_{ee}) + zk (\cos \gamma_{eo} - \cos \gamma_{ee}). \quad (15)$$

Here, k_e is the wave number for an extraordinary wave propagating perpedicularly to the optic axis, whereas k_{ee} is the wave number corresponding to an extraordinary wave that travels inside the right wedge in the direction given by β_{ee} (see Fig. 1(b)).

From Eqs. (13), (14), and (15) it is apparent that the output field consists of two plane waves (ee and eo) with different linear polarization states, propagating along different directions, and the same considerations hold as the ones made after Eq. (6).

Taking into account that, for the given optic-axis orientations and small values of α [21, 29, 30], we have

$$T_y \simeq t_{ye} t_{ee} t_{ex}^{(y)} \cos \gamma_{ee} \simeq t_{ye} t_{ee} t_{ey}^{(y)} \simeq t_{ye} t_{eo} t_{ox}^{(y)} \cos \gamma_{eo} \simeq t_{ye} t_{eo} t_{oy}^{(y)}, \quad (16)$$

so that $T_y \simeq T_x$, the approximated expression of the output field reads

$$\mathbf{E}_{out}^{(y)}(x, z) \simeq \frac{A}{\sqrt{2}} T_y a_{ee}(x, z) \left[\begin{pmatrix} 1 \\ 1 \end{pmatrix} + \begin{pmatrix} -1 \\ 1 \end{pmatrix} \exp[-i\delta_e(x, z)] \right]. \quad (17)$$

Even in this case, at least approximately, the amplitudes of the two waves are equal and their polarizations are directed at $+45^\circ$ and -45° . Furthermore, their wave vectors form the angle $\gamma_{eo} - \gamma_{ee} \simeq -\gamma_{oe}$, that is, approximately equal to that formed by the two waves of the previous case, but in the opposite sense. This means that the polarization pattern of the output field has the same structure and period of the one obtained when the incident wave is polarized along x .

When a general (although complete) incident polarization is present at the input surface of the DWD, a linear combination of the two above solutions has to be considered. In such a case, the transmitted field will consist of (up to) four plane waves, propagating along different direction, with linear polarizations along different axes, giving rise to a more complicated polarization pattern across transverse planes. Of course, the DOP remains equal to unity everywhere.

2.3. Unpolarized input light

Here we consider the case where a completely unpolarized plane wave, propagating along the z axis, impinges on the entrance surface of the DWD. A possible way to study the propagation of a completely unpolarized plane wave is to think at the latter as the superposition of two mutually uncorrelated plane waves, carrying the same power, linearly polarized along two orthogonal axes. We choose such axes as the x and y axes of the reference frame used in the previous subsection, so that the results obtained there can be directly used.

If we denote by I_0 the intensity of the input wave and set the intensity of each component wave to $I_0/2$, the polarization matrix across the entrance surface of the device, evaluated from Eq. (2) with $\mathbf{E} = \mathbf{E}_{in}^{(x)} + \mathbf{E}_{in}^{(y)}$, takes the form

$$\hat{P}_{in} = \frac{I_0}{2} \begin{pmatrix} 1 & 0 \\ 0 & 0 \end{pmatrix} + \frac{I_0}{2} \begin{pmatrix} 0 & 0 \\ 0 & 1 \end{pmatrix} = \frac{I_0}{2} \begin{pmatrix} 1 & 0 \\ 0 & 1 \end{pmatrix}, \quad (18)$$

where the lack of correlation between the two fields allowed us to write \hat{P}_{in} as the sum of the polarization matrices pertinent to each component. The corresponding degree of polarization, from Eq. (3), turns out to be zero.

The same approach can be used for evaluating the polarization matrix and the DOP of the field propagated after the DWD. In this case, the two uncorrelated fields to be considered are the ones produced by the x and the y components of the input wave, so that the polarization matrix can be evaluated from Eq. (2) with $\mathbf{E} = \mathbf{E}_{out}^{(x)} + \mathbf{E}_{out}^{(y)}$.

Although the polarization matrix at the exit of the DWD can be obtained starting from the more general formulae in Eqs. (6) and (13), a simpler expression can be derived considering the approximated Eqs. (11) and (17) for the exiting fields. Taking into account the fact that the two fields are mutually uncorrelated, the following matrix elements are obtained for $\hat{P}_{out}(x, z)$:

$$P_{out,xx}(x, z) = \frac{I_0}{4} [2 + \cos \delta_o(x, z) - \cos \delta_e(x, z)], \quad (19)$$

$$P_{out,xy}(x, z) = P_{out,yx}^*(x, z) = \frac{I_0}{4} i [\sin \delta_o(x, z) + \sin \delta_e(x, z)], \quad (20)$$

$$P_{out,yy}(x, z) = \frac{I_0}{4} [2 - \cos \delta_o(x, z) + \cos \delta_e(x, z)], \quad (21)$$

where a lossless DWD has been considered ($T_y = T_x = 1/\sqrt{2}$). The corresponding Stokes vector at a point after the DWD turns out to be, from Eq. (4),

$$\mathbf{s}(x, z) = \frac{I_0}{2} \begin{pmatrix} 2 \\ \cos \delta_o(x, z) - \cos \delta_e(x, z) \\ 0 \\ -\sin \delta_o(x, z) - \sin \delta_e(x, z) \end{pmatrix}, \quad (22)$$

with constant intensity and DOP given by

$$p_{out}(x, z) = \left| \sin \left[\frac{\delta_o(x, z) + \delta_e(x, z)}{2} \right] \right|. \quad (23)$$

Equation (22) represents the sum of the Stokes parameters corresponding to the output of the x and y components of the incident field. Since such contributions form two different periodic polarization patterns at any z plane with approximately the same transverse period, they give rise to a periodic structure both in x and z directions. This behavior can be observed in Fig. 2(a) and (b) where $s_1(x, z)$ and $s_3(x, z)$ Stokes parameters are represented. Both $s_1(x, z)$ and $s_3(x, z)$ show the same behavior with a quarter-period delay in the x direction.

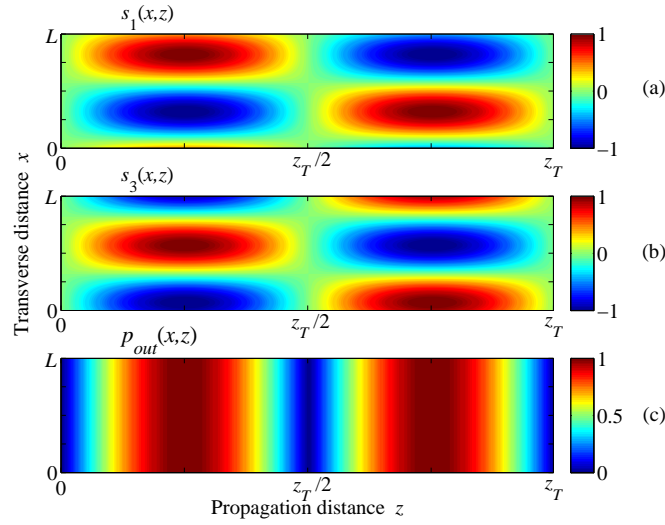


Fig. 2. Theoretical behaviors of the Stokes parameters s_1 and s_3 , normalized to the input intensity I_0 , and the degree of polarization p_{out} across the xz plane at the exit of a DWD for an unpolarized input plane wave ($s_0(x, z) = I_0$ and $s_2(x, z) = 0$).

Somewhat unexpected results can be observed in Fig. 2(c), where the DOP after the DWD is reported: i) the DOP is seemingly constant in the transverse direction at any z plane (diversely to what happens with $s_1(x, z)$ and $s_3(x, z)$) and ii) the DOP at the exit of the "depolarizer" varies from zero to one with the propagation distance, in a periodic way. This means that, for a totally unpolarized input light, the field is perfectly polarized at some transverse planes at the exit of the device.

The above characteristics of the DOP can be easily explained by further approximating the expressions of the phases δ_o and δ_e appearing in Eq. (23). In fact, retaining only the terms up to the second order in α , the phases in Eqs. (8) and (15) can be written as

$$\delta_o(x, z) \simeq kd_2(n_e - n_o) - kx(n_e - n_o)\alpha - kz(n_e - n_o)^2\alpha^2/2, \quad (24)$$

$$\delta_e(x, z) \simeq -kd_2(n_e - n_o) + kx(n_e - n_o)\alpha - kz(n_e - n_o)^2\alpha^2/2, \quad (25)$$

where n_e and n_o are the extraordinary and ordinary refractive index of the crystal. Using such an approximation, the Stokes vector becomes

$$\mathbf{s}(x, z) \simeq I_0 \begin{pmatrix} 1 \\ \sin \left[kz(n_e - n_o)^2\alpha^2/2 \right] \sin [k(n_e - n_o)(d_2 - \alpha x)] \\ 0 \\ \sin \left[kz(n_e - n_o)^2\alpha^2/2 \right] \cos [k(n_e - n_o)(d_2 - \alpha x)] \end{pmatrix}. \quad (26)$$

and the DOP of the light after the DWD turns out to be

$$p_{out}(x, z) \simeq \left| \sin \left[kz(n_e - n_o)^2\alpha^2/2 \right] \right|, \quad (27)$$

i.e., it is independent of the lateral variable x and varies from zero to one in a periodic way as a function of the propagation distance z .

At distances

$$Z_m \simeq \frac{\lambda(2m+1)}{2(n_e - n_o)^2 \alpha^2}, \quad (28)$$

behind the DWD (being $m = 0, 1, 2, \dots$), the DOP reaches its maximum value, equal to unity. There, totally polarized light field is obtained. Note that at such distances, $s_1(x, Z_m)$ and $s_2(x, Z_m)$ are sinusoidal functions of variable x with maximum amplitude. On the other hand, for distances

$$z_m \simeq \frac{\lambda m}{(n_e - n_o)^2 \alpha^2}, \quad (29)$$

$s_1(x, z_m) = s_2(x, z_m) = 0$ and the DOP vanishes, so that the field is completely unpolarized across such planes. It must be noted that consecutive z -planes where DOP is maximum and minimum are separated by the distance $Z_m - z_m = z_T/4$.

3. Experiment

In order to check the previous theoretical results, the experimental setup sketched in Fig. 3 was arranged. To synthesize the incident unpolarized light, two He-Ne lasers ($\lambda = 632.8$ nm), linearly polarized along the vertical (y) direction, were used. At the output of one of these lasers a half-wave plate (HWP) rotated at 45° was placed to obtain a linear polarization along the horizontal (x) axis. A neutral density filter (F) was used to adjust the output power of one of the lasers. The two beams were combined by using a polarizing beam splitter (PBS) and expanded by means of a telescope (a $20\times$ microscope objective MO and a collimating lens L with 200 mm focal length). The resulting wave (unpolarized and approximately plane) was sent onto a DWD. The latter (Thorlabs, DPU-25-A) consisted of two quartz wedges ($n_o = 1.5426$, $n_e = 1.5517$) [31], with nominal wedge angle $\alpha = 2^\circ$. A more precise value of α was measured by analyzing the propagated pattern in the far zone, giving $\alpha = 2.17^\circ$.

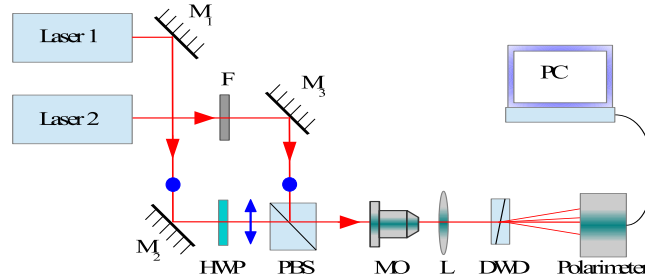


Fig. 3. Experimental setup: M_i , mirrors; F, neutral density filter; HWP, half wave plate; PBS polarizing beam splitter; MO, microscope objective; L, lens. Blue arrow and dots represent polarization directions

The degree of polarization p_{out} and the Stokes parameters of the output field were measured by means of a polarimeter (Thorlabs PAX5710VIS-T-TXP) at different x positions, at several distances from the exit surface of the DWD. The detection surface of the polarimeter was circular with diameter of $300 \mu\text{m}$.

First of all, it was checked that p_{out} was practically constant (within 5%) across the transverse direction for all z planes (see Fig. 4). The measured DOP dependence on the propagation

distance is represented in Fig. 5 (dots), together with the theoretical curve (solid line), calculated from Eq. (27). It can be observed that, at the exit of the DWD, the measured DOP is nearly zero, but it grows as the light propagates and reaches a maximum value, near unity, for a propagation distance around 2.75 m. Around this distance, the light is nearly totally polarized. Then, the DOP decreases to nearly zero when the propagation distance is around 5.5 m. This behavior is periodically repeated with increasing propagation distance. A complete agreement between calculated curve and experimental points is obtained.

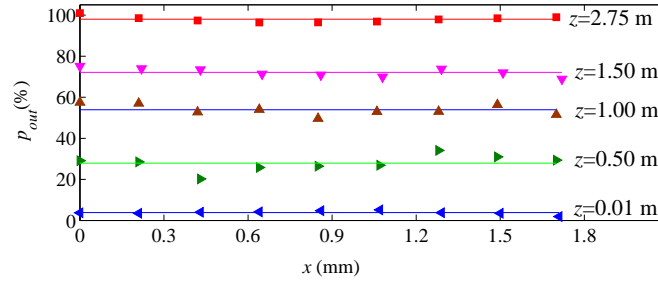


Fig. 4. Measured values of the DOP as a function of transverse displacement for several planes after the DWD when an unpolarized plane wave impinges on the DWD.

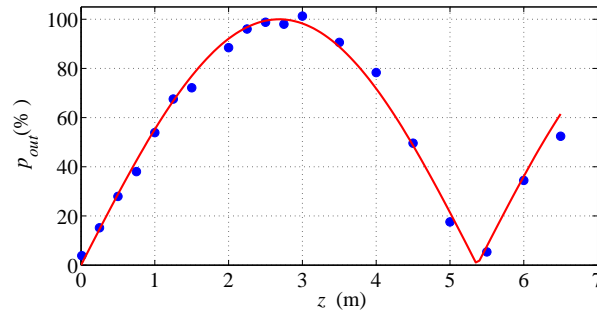


Fig. 5. Experimental and theoretical DOP as a function of the free space propagation distance after the DWD when an unpolarized plane wave impinges on the DWD.

Figure 6 shows the measured $s_1(x, z)$, $s_2(x, z)$ and $s_3(x, z)$ Stokes parameters (normalized to the total intensity I_0) at transverse planes located at different z distances behind the DWD (red circles: s_1 ; green down triangles: s_2 ; blue up triangles: s_3). At $z = 0.01$ m, the all three Stokes parameters are approximately zero, representing unpolarized light. For $z = 0.50$ m, the Stokes parameters $s_1(x, z)$ and $s_3(x, z)$ follow sinusoidal dependences vs the transverse variable x (with 0.28 maximum amplitude and a quarter-period delay), while $s_2(x, z) \approx 0$. Similar results are observed for $z = 1.50$ m and $z = 2.75$ m but with larger maximum amplitude (0.72 and 0.97, respectively) than in the previous case. Theoretical curves obtained by means of Eq. (26) are also represented for these distances. A very good agreement with experimental data is observed.

4. Conclusions

DWD's are optical devices used when a reduction of the DOP of light is required. Being deterministic objects, they are actually *pseudo-depolarizers* and their effect is to produce a periodic

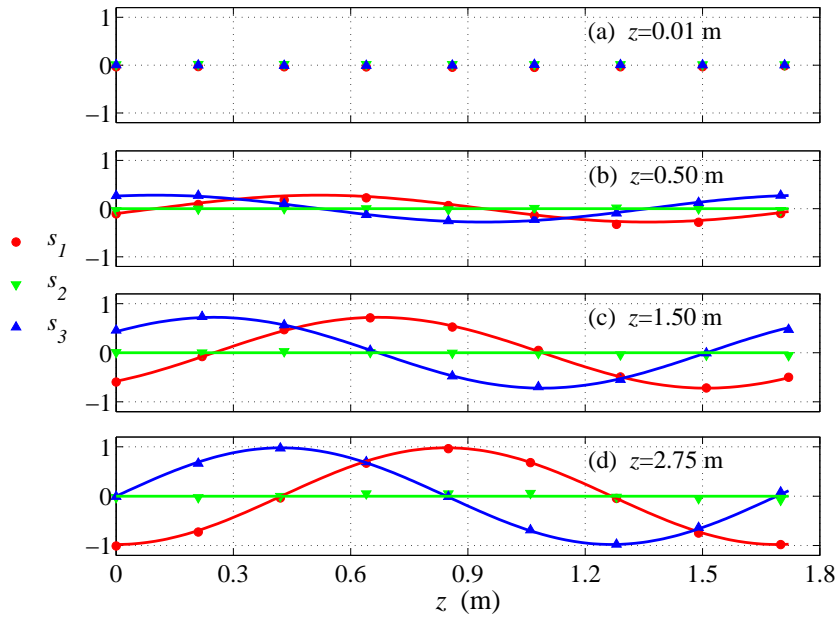


Fig. 6. Measured Stokes parameters (symbols) of the exiting light at several z -planes when an unpolarized plane wave impinges on the DWD. Calculated values (solid lines) are also represented at $z = 0.50$, $z = 1.50$, m and at $z = 2.75$ m. All values are normalized to the input intensity I_0 .

transverse variation of the polarization state of the field at their output, as the one produced by a polarization grating. As a consequence, the DOP of the output field, evaluated averaging the Stokes parameters over a sufficiently large area, turns out to be nearly zero.

In this paper, the polarization characteristics of the field produced when an unpolarized plane wave passes through a DWD have been analyzed. One of the obtained results is that, although the output field presents a periodic variation of its polarization state, the (local) DOP is uniform across any transverse plane. Furthermore, the DOP at the exit face of the DWD is zero, but it changes periodically on increasing the distance from the device. In particular, it becomes unitary at a distance corresponding to a quarter of the Talbot distance pertaining to the period of the polarization pattern produced by the DWD. The origin of such behavior arises from the superposition of two mutually uncorrelated transversally periodic polarization patterns. An experiment has been carried out to confirm the theoretical predictions.

The above properties of the DOP are exactly expected when the incident field is an ideal plane wave, and without any transverse limitations of the device. In a real experiment, the oscillating behavior of the DOP is expected only within a finite range of distances, corresponding to the region where the different fields emerging from the device overlap. Nonetheless, such a range is of the order of some tens of meters long for a typical DWD, so that several periods of the DOP oscillation can be observed.

Finally it should be noted that DWD's could be used for generating periodic polarization structures, whose DOP can be varied at will, on changing the propagation distance beyond the device.

Appendix

In this appendix, the expressions of the fields at the exit of the DWD are derived. Three-dimensional fields with generally nonvanishing z components are considered, so that the field of a plane wave, linearly polarized along x , normally incident on the DWD can be written as

$$\mathbf{E}_{in}^{(x)}(x_i, -d) = A \begin{pmatrix} 1 \\ 0 \\ 0 \end{pmatrix}, \quad (30)$$

where A is its amplitude and x_i is the x -coordinate across the entrance surface of the device.

The phase of the field at a typical point $(x, z > 0)$ at the exit of the DWD is obtained by evaluating the optical path length along the line sketched in Fig. 1(b), which represents a flux line of the wave vector inside the crystal. The amplitude of the field is derived using the transmission coefficients pertinent to every interface along the optical path.

From simple geometrical considerations, the following relation can be derived between the transverse coordinate of the optical path beyond the device and the corresponding one at its entrance surface:

$$x_i = \frac{x - z \tan \gamma_{oe} - d_2 \tan \beta_{oe}}{1 - \tan \alpha \tan \beta_{oe}}. \quad (31)$$

After propagating along the distance $(d_1 + x_i \tan \alpha)$ inside the first wedge as an ordinary wave, the field becomes

$$\mathbf{E}_{xo}^{(x)}(x_i, -d_2 + x_i \tan \alpha) = A t_{xo} \begin{pmatrix} 1 \\ 0 \\ 0 \end{pmatrix} \exp[-ik_o(d_1 + x_i \tan \alpha)]. \quad (32)$$

At the interface between the two crystals, this wave splits into an ordinary wave (oo) and an extraordinary wave (oe). The corresponding Snell's laws are

$$k_o \sin \alpha = k_o \sin(\beta_{oo} + \alpha), \quad (33)$$

$$k_o \sin \alpha = k_{oe} \sin(\beta_{oe} + \alpha). \quad (34)$$

The oo wave propagates along the z axis up to the exit surface of the device, where the field turns out to be

$$\mathbf{E}_{oo}^{(x)}(x_i, z = 0^-) = A t_{xo} t_{oo} \begin{pmatrix} \cos(\pi/4) \\ -\sin(\pi/4) \\ 0 \end{pmatrix} \exp(-ik_o d), \quad (35)$$

and after the exit surface it becomes

$$\mathbf{E}_{oo}^{(x)}(x, z > 0) = \frac{A}{\sqrt{2}} t_{xo} t_{oo} \begin{pmatrix} t_{ox}^{(x)} \\ -t_{oy}^{(x)} \\ 0 \end{pmatrix} \exp(-ik_o d - ikz). \quad (36)$$

On the other hand, the oe field across the inner side of the exit DWD face is [29, 30]

$$\mathbf{E}_{oe}^{(x)}(x_{oe}, z = 0^-) = A t_{xo} t_{oe} \begin{pmatrix} e_{oe,x} \\ e_{oe,y} \\ e_{oe,z} \end{pmatrix} \exp \left[-ik_o(d_1 + x_i \tan \alpha) - ik_{oe} \frac{(d_2 - x_i \tan \alpha)}{\cos \beta_{oe}} \right], \quad (37)$$

where $x_{oe} = d_2 \tan \beta_{oe} + x_i(1 - \tan \alpha \tan \beta_{oe})$ and $(e_{oe,x}, e_{oe,y}, e_{oe,z})^T$ (with the superscript T denoting transpose) is a unitary vector perpendicular to the oe ray vector that lies in the plane

formed by the second crystal optic axis and the wave vector of the *oe* wave. The angle β_{oe} is obtained from Eqs. (9) and (34), taking into account that $\cos \varphi_{oe} = \frac{1}{\sqrt{2}} \sin \beta_{oe}$ (see the optic axis orientation in Fig. 1(a)). Finally, the *oe* field propagating beyond the DWD turns out to be

$$\begin{aligned} \mathbf{E}_{oe}^{(x)}(x, z > 0) &= \frac{A}{\sqrt{2}} t_{xo} t_{oe} \begin{pmatrix} t_{ex}^{(x)} \cos \gamma_{oe} \\ t_{ey}^{(x)} \\ t_{ex}^{(x)} \sin \gamma_{oe} \end{pmatrix} \\ &\times \exp \left[-ik_o (d_1 + x_i \tan \alpha) - \frac{ik_{oe} (d_2 - x_i \tan \alpha)}{\cos \beta_{oe}} - \frac{ikz}{\cos \gamma_{oe}} \right], \end{aligned} \quad (38)$$

where the refraction angle γ_{oe} is obtained on applying the Snell's law at the exit surface. On replacing the x_i value given in Eq. (31), the latter equation becomes

$$\begin{aligned} \mathbf{E}_{oe}^{(x)}(x, z > 0) &= \frac{A}{\sqrt{2}} t_{xo} t_{oe} \begin{pmatrix} t_{ex}^{(x)} \cos \gamma_{oe} \\ t_{ey}^{(x)} \\ t_{ex}^{(x)} \sin \gamma_{oe} \end{pmatrix} \\ &\times \exp(-ik_o d_1 - id_2 k_{oe} \cos \beta_{oe} - ixk \sin \gamma_{oe} - izk \cos \gamma_{oe}). \end{aligned} \quad (39)$$

If the z component of the above field is neglected, the superposition of the *oo* and *oe* waves in Eqs. (36) and (39) gives the field in Eq. (6).

Following an analogous procedure, but with an incident plane wave linearly polarized along y , it is found that

$$\begin{aligned} \mathbf{E}_{eo}^{(y)}(x, z > 0) &= \frac{A}{\sqrt{2}} t_{ye} t_{eo} \begin{pmatrix} -t_{ox}^{(y)} \cos \gamma_{eo} \\ t_{oy}^{(y)} \\ -t_{ox}^{(y)} \sin \gamma_{eo} \end{pmatrix} \\ &\times \exp(-ik_e d_1 - ik_o d_2 \cos \beta_{eo} - ikx \sin \gamma_{eo} - ikz \cos \gamma_{eo}), \end{aligned} \quad (40)$$

as the output field for the *eo* wave, and

$$\begin{aligned} \mathbf{E}_{ee}^{(y)}(x, z > 0) &= \frac{A}{\sqrt{2}} t_{ye} t_{ee} \begin{pmatrix} t_{ex}^{(y)} \cos \gamma_{ee} \\ t_{ey}^{(y)} \\ t_{ex}^{(y)} \sin \gamma_{ee} \end{pmatrix} \\ &\times \exp(-ik_e d_1 - ik_{ee} d_2 \cos \beta_{ee} - ikx \sin \gamma_{ee} - ikz \cos \gamma_{ee}), \end{aligned} \quad (41)$$

for the *ee* wave. Again, on assuming as negligible the z components of such fields, their superposition gives rise to the field expressed in Eq. (13).

Acknowledgments

One of the authors (J. C. G. S.) is grateful to a grant from 2011 Fundación Caja Madrid Program. J. C. G. S. and G. P. acknowledge the hospitality of Prof. F. Gori's group.